STEPWISE CONFORMATION TRANSITIONS FOR A SEMI-STIFF RING POLYMER CONFINED IN A CONICAL TRAP INDUCED BY THE INCREASING EXTERNAL FIELD OR BY CONE'S OPENING ANGLE VARIATION

[1]A. Siretskiy, [2]C. Elvingson, [3]P. Vorontsov-Velyaminov

[1]Dept. of Informational Technology, SE-751 05, Uppsala University, Uppsala, Sweden

[2]Dept. of Chemistry, Physical Chemistry P.O. Box 523, SE-751 20, Uppsala University, Uppsala, Sweden

[3]Dept. of Molecular Biophysical, Physical Faculty, 198504, Saint Petersburg University, Saint-Petersburg, Russia

alexey.siretskiy@it.uu.se, christer.elvingson@kemi.uu.se, voron.wgroup@gmail.com

In this paper a stepwise compaction process of a ring semi-stiff polymer chain placed in a 3d conical nano-cavity and being under the action of the increasing external field is studied. Compaction from a circle-like shape to several toroidal-like loops for a three-dimensional system was observed. The thermodynamic stability of these toroidal-like structures was investigated by observing a hysteresis of the compaction-extension curves. This study extends our previous work [1] with investigation of the effect of the cone opening angle variation on the distinct shape transitions.

Keywords: semi-stiff ring polymers, Monte Carlo, compact structures, shape transitions, confinement, nanocone.

1. Introduction

It is well known, that confinement can crucially influence the conformational properties of macromolecules [2–4]. The accessible space could be reduced by a spherical cavity [5], a cylindrical pore [6], or a rectangular or circular slit [7]. In all cases, the confinement strongly affects the conformation of the molecule. An important example is the compaction of DNA which has been studied using various methods. It is accomplished for instance by adding of spermin^{+4}, spermidin^{+3} or other highly charged counterions [8, 9]. Microchannels were also used to observe the conformational changes of a single DNA molecule. It has further been found that adding a "crowding agent" also induces compaction for a semi-stiff molecule like DNA [10]. An exhaustive review of the equilibrium behavior of isolated macromolecules confined in cavities of various geometries can be found in [11] and an overview of their dynamical properties is presented in [12]. New types of nanostructures are constantly being obtained synthetically and are also found in biological systems. Specific examples include carbon nano-cones as well as conical cores in some viruses, e.g. the HIV-1 virus encapsulating its RNA content in a conical confinement [13, 14]. Well defined synthetic carbon nano-cones can also be produced during pyrolysis of hydrocarbons [15]. Such conical structures can be used to investigate the role

of non-uniform confinement on the stability of e.g. toroidal structures formed by semi-stiff ring polymers, such as DNA.

In this work we investigate how the shape of such a nano-cone will affect the structure of a ring polymer during non-uniform confinement by introducing an external field in the direction toward the tip of the cone. By varying strength of the external field, acting on the polymer, the volume effectively accessible by the polymer will change. It is possible thus to imitate different cone heights in a single computer simulation. Studying stability of several structuresformed during confinement, can provide us better understanding of the structure of RNA(DNA) confined in differently shaped viral capsids, or the properties of synthetic and biopolymers in artificially fabricated confinements.

Simulations are performed in the canonical ensemble within conventional Metropolis Monte Carlo(MC) [17]. Our interest is in the conformational properties of a *semi-stiff chain*, and we show that for the special kind of confinement used here, the external field is able to induce several shape transitions of the semi-stiff polymer in three-dimensions. It should also be mentioned that in the case of the two-dimensional slit, the similar looping with the thermodynamically stable conformations were observed in the computer experiment [1].

The possibility for a semi-stiff circular polymer to have stable looped conformations are shown also analytically using simplifying assumptions. Further, we investigate the relative stability of the polymer at different degrees of compaction as a function of the external field strength. To reveal the role of the shape of the confinement we run simulations for constant external field strength but varying the cone opening angle.

In section 2 we describe the model, in section 3 we introduce the computational methods, and in section 4 the results are presented. The conclusions are made in section 5.

2. Model

The ring polymer consists of N beads connected by N bonds, where the bond length was allowed to fluctuate. We thus include the following interactions in our model: 1) bond stretching, 2) bending rigidity (characterized by the angle between consecutive bonds), 3) repulsion from the wall, confining the polymer, 4) an external potential acting on the center of mass of the polymer, and 5) Lennard-Jones (LJ) interactions between the nonbonded beads. The direction of the external field was chosen to decrease the potential energy of the chain when moving towardsthe towards the cone tip.

So the Hamiltonian of the system is presented as:

$$H = E_{stretch} + E_{bend} + E_{exc} + E_{ext} + E_{LJ}, \tag{1}$$

where $E_{stretch}$ is the energy due to bond length fluctuation, E_{bend} is the bending energy, E_{exc} is the wall repulsion, E_{ext} is the external field contribution, and E_{LJ} is the Lennard-Jones potential included in the three-dimensional case.

Specifically for a chain with N beads, $E_{stretch}$ was calculated using a FENE-type [16] (finitely extensible non-linear elastic) potential:

$$E_{stretch}(b) = \begin{bmatrix} -\gamma \sum_{i=1}^{N} \ln \left[1 - \left(\frac{b_i - b_0}{\Delta b_{max}} \right)^2 \right] & , & |b_i - b_0| \leqslant \Delta b_{max} \\ \infty & , & |b_i - b_0| > \Delta b_{max}, \end{bmatrix} \tag{2}$$

where γ is the stretching constant, Δb_{max} is the maximal bond length fluctuation, $b_i = |\mathbf{b}_i|$, and where $b_0 = |\mathbf{b}_0|$ is the equilibrium bond length. Within the equilibrium length region

the FENE behaves similar to the harmonic potential, but unlike the latter it does not allow infinite bond extension. The bending energy is given by

$$E_{bend}(\theta) = \kappa \sum_{i=1}^{N} (1 - \cos\theta_i),$$ (3)

where $\theta_i = \widehat{\mathbf{b}_i, \mathbf{b}_{i+1}}$ is the angle between successive bond vectors $\mathbf{b}_i$ and $\mathbf{b}_{i+1}$ (or between bond vectors $\mathbf{b}_N$ and $\mathbf{b}_1$ for $i = N$), and κ characterizes the bending stiffness. The confining walls were considered to be hard walls, characterized by:

$$E_{exc} = \left[\begin{array}{l} 0, \text{ all beads are inside the cone} \\ \infty, \text{any of N beads is outside the cone,} \end{array} \right.$$ (4)

The interaction with an external force field is given by

$$E_{ext}(x) = \sigma z,$$ (5)

where z is the distance between the center of mass of the polymer and the cone tip, in which $z = 0$, see Fig. 1(a), σ is the constant which detemines the force of the external filed. To take into account for the excluded volume interactions, and in order to introduce attraction between the chain monomers-beads to stabilize the ring polymer during compaction we also include a LJ potential:

$$E_{LJ} = \sum_{i=1,j<i}^{N} u(r_{ij}) = 4\epsilon \sum_{i=1,j<i}^{N} \left[(a/r_{ij})^{12} - (a/r_{ij})^{6} \right],$$ (6)

where r_{ij} is the distance between bead centers, ϵ is the depth of the potential minimum, and a is the bead diameter. We found, that neglecting the attractive part in the case of three dimensions, could make structures forming toroidal loops unstable.

To simplify notation, we use dimensionless units throughout. The energy is measured in the units of ϵ: $H = \epsilon H^*$. Distances are given in units of b_0: $b^* = b/b_0$. The bead size is set to be equal to $a = 0.1b_0$, and the maximal bond fluctuation is $\Delta b_{max} = 0.5b_0$. The units of the reciprocal dimensionless temperature β^* is obtained from the relation: $H\beta = H^*\beta^*$, where $\beta = 1/k_B T$ and $\beta^* = 1/T^*$.

The values of the bending constant, κ, the stretching constant γ, and the magnitude of the external field σ are chosen to maintain the property of a (semi)stiff chain, but still flexible enough to show shape transitions. The persistence length, l_p, was equal to $10b_0$. For a chain with $N = 20$, this means that the contour length is approximately $2l_p$. The relation between the bending force constant and the persistence length is given in the Appendix.

3. Method

The Metropolis Monte Carlo method (MC) in the canonical ensemble [17] was used to investigate the equilibrium properties of the system. One MC step corresponding to a single bead displacement or a flip of a segment of the chain (crankshaft move), is presented in Fig. 1(b).

The chain length of $N = 20$ was chosen to investigate shape transitions. The frequency of the crankshaft moves to the single bead displacements were in this case from 1:10 up to 1:1. Our observation has shown that proposed frequency ratio is enough for chain to relax after a large conformational change corresponding to a segment flip. The flip segment length was uniformly chosen in the interval $[1:15]$.
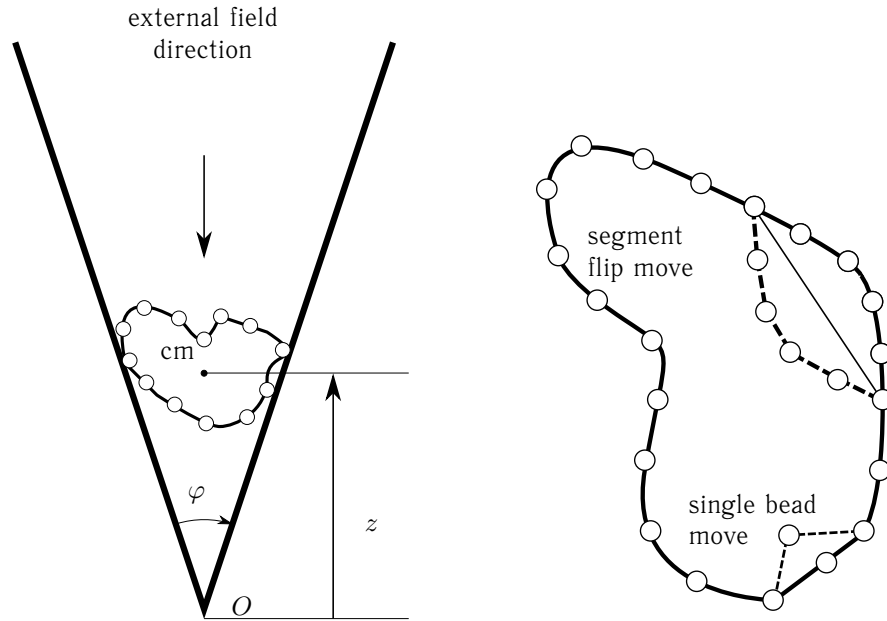
Fig. 1. (a) A sketch of the system used in the simulations. The position of the center of mass of the polymer is denoted by "cm", and "z" is the distance between the level of the "cm" and the tip of the cone, O, and φ is the cone opening angle. (b) Illustration of the possible moves. The trial configuration for a single bead displacement and for a segment flip (crankshaft move) are shown as dashed curves

The transition probability to accept a trial move is the conventional Metropolis criterion [17]:

$$acc[o \rightarrow n] = \min[1, e^{-\beta \Delta H}], \tag{7}$$

where $\Delta H = H(n) - H(o)$ and n and o denote the new and the old configurations respectively.

4. Results

4.1. External field dependence

In order to understand a possibility for a semi-stiff ring polymer to form stable looped structures in the nonuniform confinement, it is feasible to consider a simplification of the proposed model, and evaluate *phantom* semi-stiff ring polymer. That is we drop the Lennard-Jones contribution (6) and therefore allowing the monomers to intersect, while preserving the confining walls interactions (4). All the angles between the monomers θ and all the bond lengths b for all monomers are considered equal, bond length fluctuations are not considered. Under these restrictions the possible conformations are circular, made of integer number of loops.

The Hamiltonian (1) then is reduced to:

$$H = E_{stretch} + E_{bend} + E_{exc} + E_{ext}, \tag{8}$$

It is possible to rewrite the Hamiltonian contributions as functions of z with parameter λ, where z is the distance between the level of the top of the cone and the level of
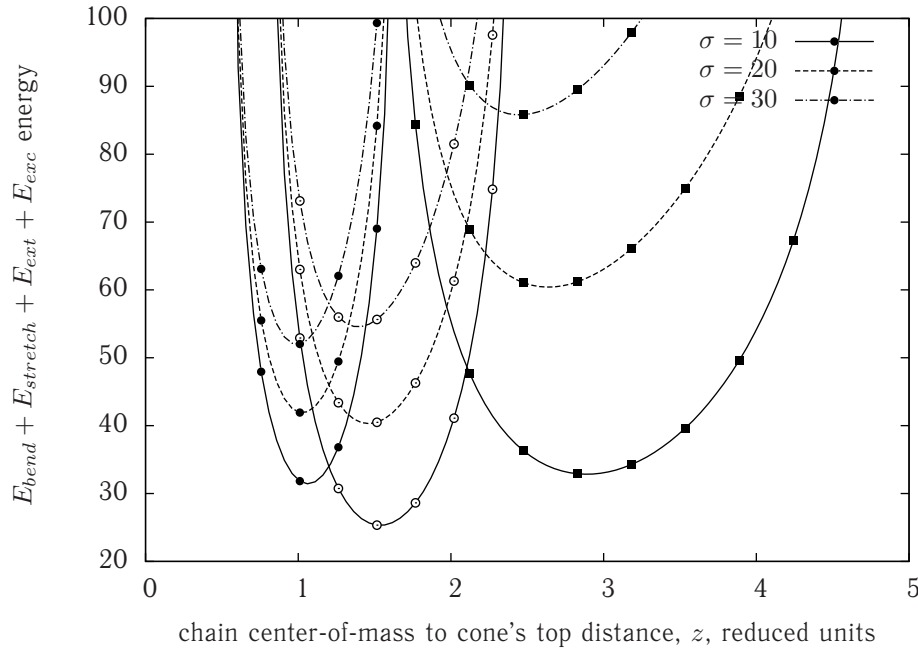
Fig. 2. Analytical curves according to (9): full chain energy H as a function of the distance between the center of mass of the chain and of the cone's tip z for different external fields amplitudes σ. Curves for different σ are marked with different line types: $\sigma = 10$ – solid, $\sigma = 20$ – dashed, and $\sigma = 30$ – dot-dashed. Different symbols denote energy curves for different number of loops: $\lambda = 1$ – filled squares, $\lambda = 2$ – open circles, $\lambda = 3$ – filled circles. Other parameters are: $\tan(\varphi/2) = 1$, $\gamma = 2$, $\kappa = 5$, $\Delta b_{max} = 0.5$, $N = 20$

center of mass (Fig. 1) of the one, two and three loops formed by the ring polymer, and λ is the number of loops:

$$H(z; \lambda) = -N\gamma \ln \left[1 - \frac{1}{\Delta b_{max}^2} \left(2 \sin \frac{\lambda \pi}{N} \tan(\varphi/2)z - 1 \right)^2 \right] + 2\kappa N \sin^2 \frac{\lambda \pi}{N} + \sigma z. \qquad (9)$$

The curves of the (9) for $\lambda = 1, 2, 3$ in Fig. 2 show, how the external field, given by (5) can induce energetically stable loops with the increase of the field amplitude $\sigma = 10, 20, 30$.

For each line type there are three energy wells, marked with different point types, with the minima positions revealing the distances between the cone's top and the mass center position for $\lambda = 1, 2, 3$ looped structures. One can see, for example, that for $\sigma = 10$, the energy minimum for $\lambda = 2$ (open circles) is lower than for $\lambda = 1$ (filled squares). But at the same time, the energy minimum for $\lambda = 3$ (filled circles) is *higher* than for $\lambda = 2$ (open circles), showing that the three looped structure is less energetically favourable than the two looped one. Situation though changes with the external field strengthens, and for $\sigma = 30$ the three looped structure has a lower energy than the two looped one, providing for the looped structure to be *thermodynamically* stable.

The repulsive part of the LJ interactions provides excluded volume interactions, while the attractive part will add a stabilizing contribution to any compact configuration.

In Fig. 3, we first show the screenshots of the semi-stiff ring polymer in three dimensions at different stages of compaction.
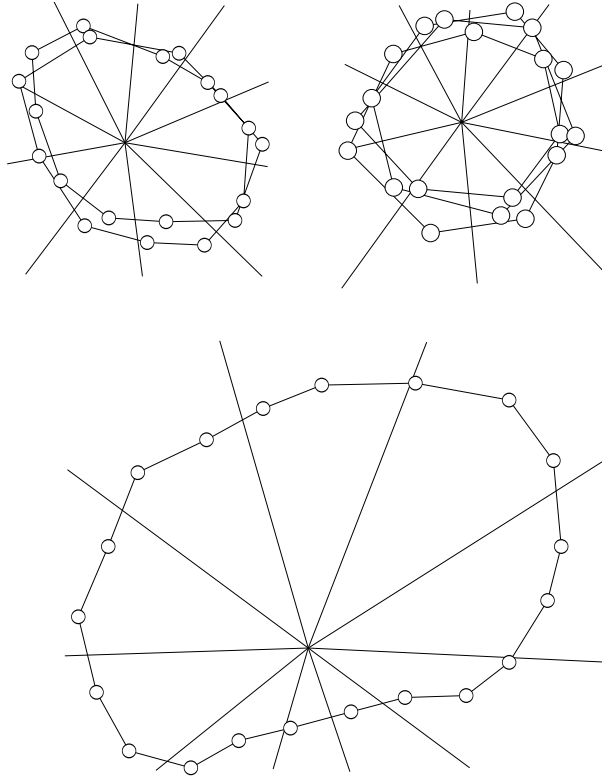

Fig. 3. Examples of different stages of compaction: from 1 to 3 loops. The view is from the top and the tip of the cone is at the center, while the lines originating from the tip are the generatrixes of the cone. The system shown is $N = 20$, $\varphi = \pi/2$, $\beta = 2.0$, and $\gamma = 2.0$, and $\kappa = 5.0$.

To demonstrate the stability of the ring polymer with 2 or 3 loops, we show in Fig. 4 the radius of gyration R_g as a function of the external field strength σ during the compaction process $(1 \rightarrow 2 \rightarrow 3)$ loops and the expansion process $(3 \rightarrow 2 \rightarrow 1)$. In Fig. 4, one can clearly observe a hysteresis in the radius of gyration with respect to the external field strength. It is possible to interpret the hysteresis curves as follows: a stronger external field is needed to produce *compaction*, than to *expand* a ring polymer with the same amount of loops.

In Fig. 4 we also show $R_g(\sigma)$ for different temperatures. One can see that the lower is the temperature, the broader is the hysteresis loop. The temperature doesn't play any significant role in the region of the same amount of loops, but does effect on the value of the "threshould" σ, making the hysteresis loop broader.

The graphs can be split into three regions $\sigma \in (0 : 10)$, $\sigma \in (20 : 40)$, and $\sigma > 40$. These regions represent one, two and three loops correspondingly. Within each of the regions the curves show how the radius of gyration changes when the external field strength varies for the molecule forming one, two, and three loops respectively.
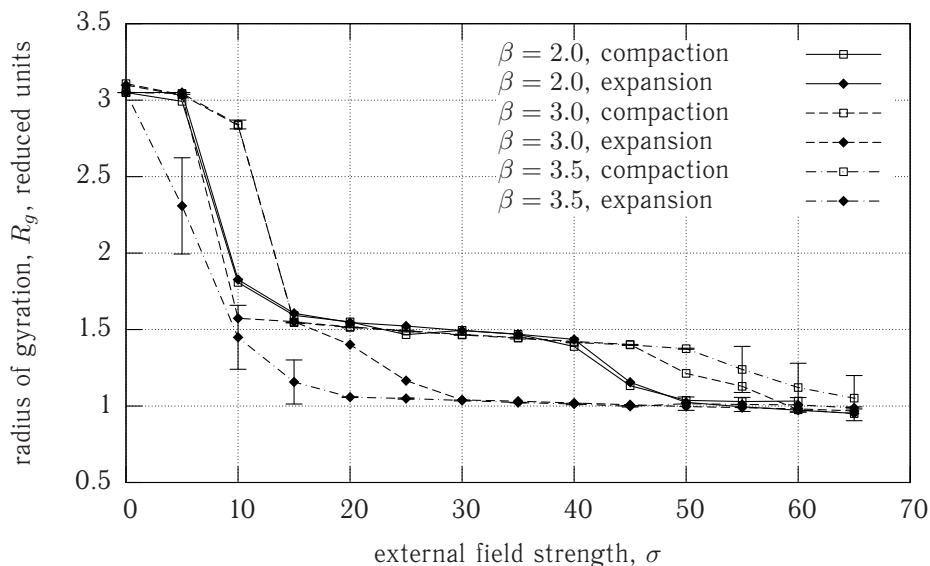
Fig. 4. Hysteresis observed during the compaction-expansion process of a semi-stiff ring polymer. The radius of gyration R_g dependence on the magnitude of the external field σ is shown for the system $N = 20$ for different inversed temperatures, $\beta = 2.0, 3.0, 3.5$ with solid, dashed and dot-dashed curves. The compaction is marked with squares, and the expansion with diamonds. The rest of the parameters are $\varphi = \pi/2$, $\gamma = 2.0$, and $\kappa = 5.0$. Some error bars are also shown.

One can consider an average "slope" of the curves for compaction to notice that the slope is decreasing, showing that with an increasing number of loops it becomes gradually harder to induce further compaction. The error bars are shown to demonstrate, that during the *compaction* of a certain structure, the fluctuations in size are small, while in the *transition region* the fluctuations are large, revealing the *cooperativity* of the transitions.

A simple analysis can also be done to show (in addition to the screenshots in Fig. 3) that the radius of gyration of these loops converges to the values, $R_g = \{3.0, 1.5, 1.0\}$ (Fig. 4) that fits very nicely, up to a scaling factor, the R_g curve for the ideal line of contour length L sequentially packed into 1, 2 and 3 loops: $R_g(k) = \frac{L}{2\pi k} \to R_g = \{3.0, 1.5, 1.0\}$, where i is the number of loops.

4.2. Opening angle dependence

As it was mentioned in [1], the orientation of the loops to the cone's axis depends on the value of the opening angle of the cone. Curves for the simplified model (8), similar to shown in Fig. 2 can be plotted for constant amplitude of the external field, σ, while varying the cone opening angle φ. Number of energetically favourable loops formed by the phantom ring polymer appears to be dependent on the cone's opening angle, φ, as shown on Fig. 5, where the energy curves for $H(z; \lambda)$ from (9) are plotted for the external field strength of $\sigma = 30$, enough to introduce compaction up to 3 loops for $N = 20$ chain, for the three different cone's opening angles: $\varphi = 120°$, $\varphi = 90°$, and $\varphi = 60°$. As one can see too "broad" cones are not very suitable for loop formation.

In order to investigate the change of the orientation of the loops depending on the opening angle we conducted MC-simulations with the full Hamiltonian (1) and observed
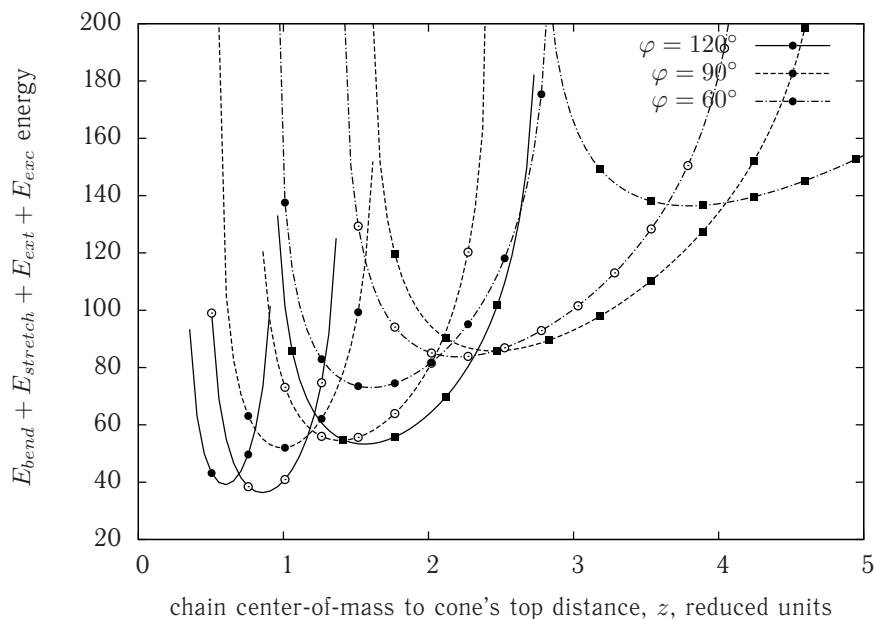
Fig. 5. Analytical curves according to (9): full chain energy H as a function of the distance between the centre of mass of the chain and the cone's tip z for different opening angles φ. Curves for different σ are marked with different line types: $\varphi = 120$ – solid, $\varphi = 90$ – dashed, and $\varphi = 60$ – dot-dashed. Different symbols denote energy curves for different number of loops: $\lambda = 1$ – filled squares, $\lambda = 2$ – open circles, $\lambda = 3$ – filled circles. Other parameters are: $\sigma = 30$, $\gamma = 2$, $\kappa = 5$, $\Delta b_{max} = 0.5$, $N = 20$.

the behaviour of a normalized to unity length vector $\mathbf{n}$ calculated as follows:

$$\mathbf{n} = \left\langle \sum_{i=1}^{N-1} (\mathbf{r}_i - \mathbf{r}_{cm}) \times (\mathbf{r}_{i+1} - \mathbf{r}_{cm}) \right\rangle, \tag{10}$$

where $\mathbf{r}_j$ – radius-vector of the bead j, $\mathbf{r}_{cm}$ – is the position of the center of mass of the chain, "$\times$" – denotes the cross-product, and the canonical ensemble averaging $\langle \cdots \rangle$ being applied. The z-component of $\mathbf{n}$ is directed along the cone's axis. So if the z-component is greater than the other two, located in the plane perpendicular to the cone's axis, then one can conclude that the loops orientation is like shown on the Fig. 3. If all of the components are close to zero due to averaging out, then the loops are oriented as in the two-dimensional case. Figure 6 shows the components length of the $\mathbf{n}$, depending on the opening angle value. It is possible to observe that in the case of strong compacting field, the orientation of the loops of the chain is perpendicular to the cone's axis up to $\varphi \approx 90^*$. After that, however, the orientation changes, that is demonstrated by the graph of the $\mathbf{z}$-component of $\mathbf{n}$. In the opening angle interval $\varphi \in (60^\circ : 90^\circ)$, the number of loops remains constant (i.e. 3), that corresponds to $R_g \approx 1$ in the reduces units, while the orientation of the loops changes, Fig. 6.

Another conclusion from Fig. 6 can be made: not only the orientation of the loops, but also the number of them is dependent on the opening angle. For the "too broad" cones no compaction is possible, since there are effectively no wall left to squeeze the ring polymer.
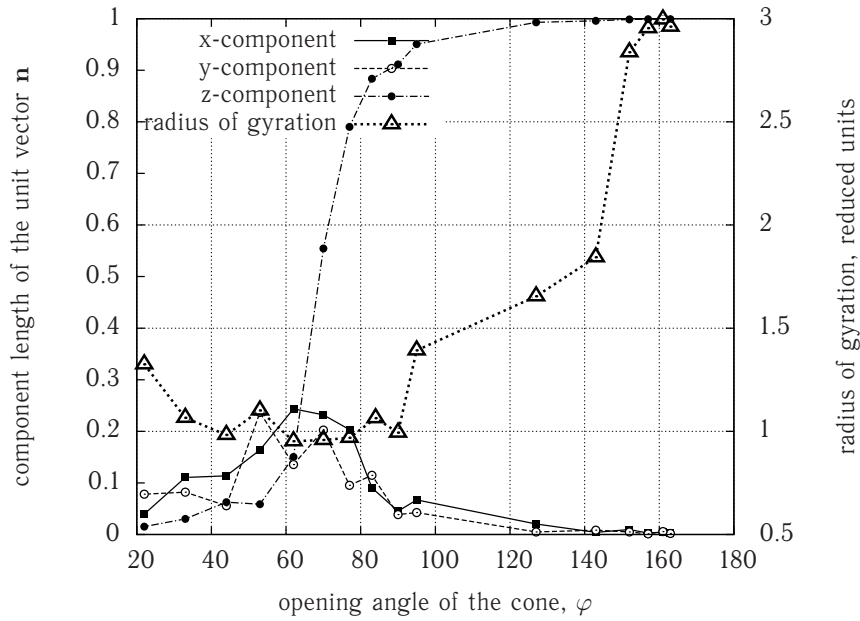
Fig. 6. Components **x**, **y**, and **z** of the unit vector **n**, (10), as a function of the opening angle, φ. Radius of gyration, R_g as a function of the φ. The system's parameters are: $N = 20$, $\gamma = 2.0$, $\kappa = 5.0$, $\sigma = 50$, and $\beta = 3.0$.

The snapshots capturing the orientation change for 3-looped structure, and an example of the irregular structure for the very narrow cone are shown on the Fig. 7.
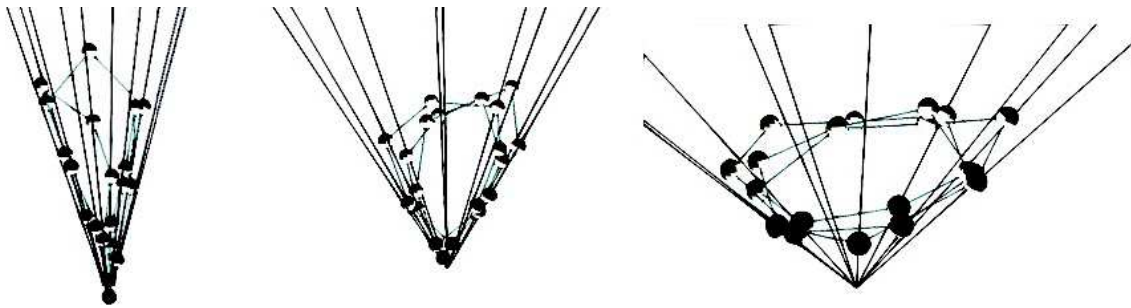

Fig. 7. Printscreens for the cone opening angle $\varphi \approx 30°$, $\varphi \approx 60°$, and $\varphi \approx 90°$ from the left to the right correspondingly. For the most narrow cone, there are no loops formed, but some irregular structure instead. The orientation of the loops changes with the grows of φ. The rest parameters as for the system in the Fig. 6

5. Conclusions

In the present communication, we continued studies of work [1] to investigate discrete shape transitions of a semi-stiff ring polymer confined in a conical trap. The proposed model of a ring polymer including chain stiffness undergoes a set of a distinct shape transitions, starting from a single loop up to several ones. The crucial role of the studied compaction is due to the a conical geometry and a direction of the external field acting on the center of mass of the chain. Such kind of shape transitions is not a specific

feature of the dimensionality of the system, as long as the same behaviour can be observed in the two-dimensional slit and in a three-dimensional conical pore.

The two ways of inducing a compaction was considered in the present work: 1) the external field σ change with fixed cone's opening angle φ, 2) and the cone's opening angle change while keeping the external field constant, but sufficient to induce compaction.

From the first hand, a theoretical possibility to form the energetically stable structures was concluded, based on the investigation of the Hamiltonian of the system looped into one, two, and three loops correspondingly.

Both of the considered ways to induce compaction lead to the looping of the semi-stiff ring polymer. The formed configurations while varying the external field strength are shown to be locally thermodynamically stable.

We investigate further the phenomenon observed earlier in [1], namely, the orientation of the loops with the opening angle change. It was shown that the orientation of the loops is changing with the value of the opening angle of the cone. The vector normal to the loop(s), **n**, as stated in (10) was used to describe the orientation of the loops.

Four regimes were detected: 1) a stick-like, then no loops can be formed in the case of too narrow cone, $\varphi \approx 30°$ 2) a narrow cone regime, with the vector **n** oriented perpendicular the cone's axis $\varphi \approx 40° \div 60°$, 3) a broad cone regime, with the vector **n** collinear to the cone's axis, $\varphi \approx 60° \div 160°$, and 4) too broad cone, when no looping is possible at all due to the effective absence of the confining walls, $\varphi > 160°$.

Acknowledgement

Appendix: persistence length derivation

The persistence length can be evaluated by first calculating the average bending angle using [18]:

$$\langle \cos\theta \rangle = \frac{\int \cos\theta \, e^{\alpha\cos\theta} ||J|| d\theta}{\int e^{\alpha\cos\theta} ||J|| d\theta}, \tag{11}$$

where $\langle \cdots \rangle$ is the canonical ensemble averaging, θ is the bond angle, and $\alpha = \kappa\beta$ is the bending stiffness constant κ in $k_B T$ units, and $||J||$ – is the determinant of the Jacobian matrix: $||J|| = r^2 \sin\theta$ for the three-dimensions.

The persistence length in terms of b_0 can then be evaluated using [19]:

$$l_p = \frac{1 - \langle \cos\theta \rangle^N}{1 - \langle \cos\theta \rangle}. \tag{12}$$

References

[1] Siretskiy A., Elvingson C. Role of non-uniform confinement in shape transitions of semi-stiff polymers. *Molecular Physics*, **113**(1), P. 1–8 (2013).

[2] Odijk T. Statics and dynamics of condensed DNA within phages and globules. *Phil. Trans. R. Soc. A*, **362**, P. 1479–1517 (2004).

[3] Choi M., Santangelo C. D. et. al., The first experimental observation of the biaxial confinement of semi-flexible filament in a channel. *Macromolecules*, **38**, P. 9882 (2005).

[4] LaMarque J. C., Le T. V. L., Harvey S. C. Packaging double-helical DNA into viral capsids. *Biopolymers*, **73**, P. 348–355 (2004).

[5] Ostermeir K., Alim K., Frey E. Buckling of stiff polymer rings in weak spherical confinement. *Phys. Rev. E.*, **81**(6), P. 1–8 (2010).

[6] Odijk T., The statistics and dynamics of confined or entangled stiff polymers. *Macromolecules*, **16**(8), P. 1340–1344 (1983).

[7] Liu Y., Chakraborty B. Shapes of semiflexible polymers in confined spaces. *Phys. Biol.*, **5**(2), P. 1–8 (2008).

[8] Yoshikawa K., Takahashi M., Vasilevskaya V., Khokhlov A. Large discrete transition in a single DNA molecule appears continuous in the ensemble. *Phys. Rev. Lett.*, **76**, P. 3029–3031 (1996).

[9] Bloomfield V. DNA condensation by multivalent cations. *Biopolymers*, **44**, P. 269–282 (1997).

[10] Zhang C., Shao P. G., van Kan J. A., van Maarel J. C. Macromolecular crowding induced elongation and compaction of single DNA molecules confined in a nanochannel. *PNAS*, **106**, P. 16651–16656 (2009).

[11] Gorbunov A. A., Skvortsov A. M., Statistical properties of confined macromolecules. *Advances in colloid and interface science*, **62**(1), P. 31–108 (1995).

[12] Milchev A. Single-polymer dynamics under constraints: scaling theory and computer experiment. *J. Phys. Cond. Matter.*, **23**(10), P. 3101 (2011).

[13] Li S., Hill C. P., Sundquist W. I., Finch J. T. Image reconstructions of helical assemblies of the HIV-1 CA protein. *Nature*, **407**, P. 409 (2000).

[14] Ganser B. K., Li S., Klishko V. Y., Finch J. T., Sundquist W. I. Assembly and analysis of conical models for the HIV-1 core. *Science*, **283**(80), P. 5398 (1999).

[15] Naess S. N., Elgsaeter A., Helgesen G., Knudsen K. D. Carbon nanocones: wall structure and morphology. *Sci. Technol. Adv. Matter.*, **10**, P. 065002 (2009).

[16] Milchev A., Binder K. Dynamics of Polymer Chains Confined in Slit-Like Pores. *J. Phys. II France*, **6**, P. 21-31 (1996).

[17] Metropolis N., Rosenbluth A., Rosenbluth M., Teller A., Teller E., Equation of State Calculations by Fast Computing Machines. *J. Chem. Phys.*, **21**(6), P. 1087–1092 (1952).

[18] Schellman J. A., Flexibility of DNA. *Biopolymers*, **13**, P. 217 (1974).

[19] Freed K. F. *Renormalization group theory of Macromolecules*. New York.: Wiley&Sons (1987).